Colloids and Surfaces A: Physicochem. Eng. Aspects 509 (2016) 190–194

Contents lists available at ScienceDirect

Colloids and Surfaces A: Physicochemical and Engineering Aspects

journal homepage: www.elsevier.com/locate/colsurfa

Enhancement of diatomite solid acidity by Al incorporation, as evaluated by the catalytic effects on the thermal decomposition of 12-aminolauric acid

Liangliang Deng[a,b], Dong Liu[a,*], Peixin Du[a,b], Hongling Bu[a,b], Yaran Song[a,b], Qian Tian[a,b], Weiwei Yuan[c], Peng Yuan[a], Zongwen Liu[d], Hongping He[a]

[a] CAS Key Laboratory of Mineralogy and Metallogeny, Guangdong Provincial Key Laboratory of Mineral Physics and Materials, Guangzhou Institute of Geochemistry, Chinese Academy of Sciences, Wushan, Guangzhou 510640, China
[b] University of Chinese Academy of Sciences, Beijing 100049, China
[c] Zhengzhou Institute of Multipurpose Utilization of Mineral Resources, Chinese Academy of Geological Sciences, Zhengzhou 450006,China
[d] School of Chemical and Biomolecular Engineering, The University of Sydney, Sydney, 2006, Australia

GRAPHICAL ABSTRACT

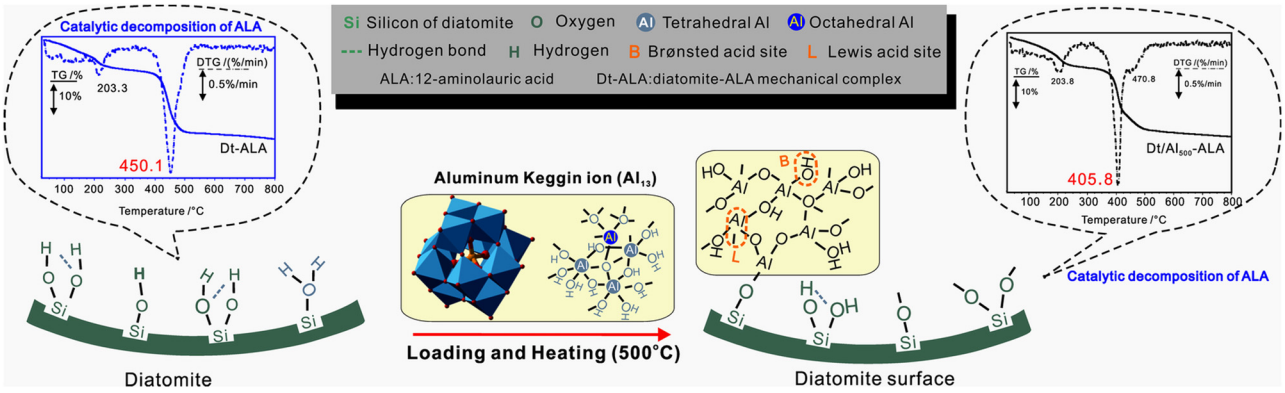

HIGHLIGHTS

- Tridecameric aluminium polymer-incorporated diatomite has high solid acidity.
- Lewis acidity of Al-incorporated diatomite is stronger than Brønsted acidity.
- Al-incorporated diatomite decreases the ALA degradation temperature by catalysis.

ARTICLE INFO

Article history:
Received 16 May 2016
Received in revised form 30 August 2016
Accepted 2 September 2016
Available online 3 September 2016

ABSTRACT

In this study, Al was incorporated into the structure of diatomite by loading tridecameric aluminium polymer and subsequently heating to improve the solid acidity of diatomite. The results show that Al incorporation increased the number of Brønsted (B) and Lewis (L) acid sites of diatomite by implanting Al-OHs and unsaturated Al^{3+} ions, respectively. L acid sites increased with the increment of preparation temperatures of Al-incorporated diatomite, whereas the B acid sites decreased. Moreover, L acid sites

* Corresponding author.
E-mail address: liudong@gig.ac.cn (D. Liu).

http://dx.doi.org/10.1016/j.colsurfa.2016.09.005

Keywords:
Al-incorporated diatomite
Solid acidity
Catalysis
12-aminolauric acid

have stronger acidity than B acid sites. Al-incorporated diatomite exhibits high catalytic activity and considerably decreases the degradation temperature of 12-aminolauric acid (ALA). Large quantities of NH_3 and CO_2 were generated, which was sourced from ALA decomposition with the catalysis of B and L acid sites, respectively; and CO_2 was obtained at a lower temperature than NH_3. The manufactured Al_{13}-diatomite composite shows promise as a solid acid catalyst.

1. Introduction

Diatomite, which is a natural biogenetic mineral, is sourced from the assemblage of the mineralized exoskeletons of diatoms [1,2]. Diatomite is primarily composed of amorphous hydrated silica ($SiO_2{\cdot}nH_2O$), which is categorized as non-crystalline opal-A, according to the mineralogical classification [3–5]. Because diatomite has macroporous structures with pore sizes that range from the nanometric to the micrometric domains [2,6], it has been widely used as adsorbents [7–11], supports [12–18], and templates of macroporous materials [2,6] [19–22].

Diatomite contains Brønsted (B) acid sites, which originate from diatomaceous silanols (Si-OHs) and exhibit weak catalytic activity [3–5]. In our previous study [20–23], the inherent solid acidity of diatomite was utilized to catalyze the decomposition of furfuryl alcohol to prepare diatomite-templated carbon with a unique macroporous structure. However, the catalytic activity of diatomite is ordinary because of the small number and weak acidity of these solid acid sites and because of the lack of Lewis (L) acid sites in the structure of diatomaceous silica. This disadvantage of the solid acidity of diatomite generally restricts the application of diatomite as a catalyst.

In our recent study [24], hydroxyl aluminium polymer (tridecameric aluminium polymer, abbreviated to Al_{13}) was incorporated into the structure of diatomite via a condensation reaction to investigate the possible mechanism of its incorporation. The solid acidity of diatomite markedly increased, and L acid sites appeared after the Al incorporation, as investigated using Fourier transform infrared (FTIR) spectroscopy. Moreover, the Al-incorporated diatomite exhibited various solid acidity values when prepared at various temperatures, which implies that it is a promising catalyst. However, until now, the properties of these new acid sites, such as their acid strength and catalytic effect, were unclear, even though such information would aid the practical application and industrial production of diatomite products.

In the present work, Al-incorporated diatomite was prepared by loading Al_{13} onto the surface of diatomite and subsequently heating the resulting composite at various temperatures. The acidity of the obtained diatomite products was investigated using temperature programmed desorption (TPD). 12-aminolauric acid (ALA; $NH_2(CH_2)_{11}COOH$) was selected as the model for evaluating the catalytic activity of the Al-incorporated diatomite. ALA contains amino and carboxyl groups and can provide simultaneous estimates of the B and L acidity of the catalyst during thermal decomposition, as previously reported [25–27].

2. Materials and methods

2.1. Diatomite

Diatomite was purchased from Sigma-Aldrich, Inc. (CAS number: 6179053-2). The dominant diatoms in diatomite were of the genus *Coscinodiscus* Ehrenberg (Centrales) and were disk-shaped, with a highly developed macroporous structure. The diatomite samples are denoted as Dt.

2.2. Preparation of Al-incorporated diatomite

Al-incorporated diatomite was prepared as follows. Al_{13} was loaded onto the surface of the diatomite, and the obtained diatomite-Al_{13} composite was subsequently heated. Heating was performed in a programmable temperature-controlled muffle oven at 250, 350 or 500 °C for 3 h. The obtained samples were ground into powder in an agate mortar; they are denoted hereafter as Dt/Al_{250}, Dt/Al_{350} and Dt/Al_{500}, respectively.

The structure, morphology and macroporosity of the diatomite before and after the Al incorporation are described in our previous report [24].

2.3. Measurement of the solid acidity of diatomite and its Al-incorporated products

The acidity of diatomite and its derivative was investigated using the NH_3-TPD method. The TPD analysis was performed using a TP 5000-II multiple adsorption apparatus (Tianjin Xianquan Corporation of Scientific Instruments, China). Approximately 100 mg of diatomite and its Al-incorporated products were pretreated under an argon atmosphere at 60 °C for 1 h. When the mass baseline was stable, the argon flow was stopped and NH_3 was introduced until the adsorption of the samples was saturated. The sample chamber was then purged with argon to remove residual NH_3 from samples' surfaces. The samples were then heated under flowing argon to 600 °C at a rate of 10 °C/min for NH_3 desorption. The desorbed gas was monitored using a mass spectrometer (Hiden QIC-20) by tracking the $m/z = 15$ mass-to-charge signal with subsequent numerical integration.

2.4. Evaluation of the catalytic activity of diatomite and its Al-incorporated products

The catalytic activity was evaluated on the basis of the thermal behaviors of ALA in the presence of diatomite and its derivatives using a thermogravimetry (TG) instrument. First, 10 g of diatomite and its derivatives were mixed with 2.5 g of ALA; they were then ground by ball milling for 20 min using a Pulverisette-6 planetary mill. These ALA-diatomite complexes are denoted as Dt-ALA, Dt/Al_{250}-ALA, Dt/Al_{350}-ALA, and Dt/Al_{500}-ALA according to the Dt and Al-incorporated products.

The TG analysis of the samples was performed on a Netzsch 449C instrument. Approximately 20 mg of finely powdered samples was heated from 30 to 1000 °C at a heating rate of 10 °C/min under a high-purity N_2 atmosphere (60 cm^3/min).

Gaseous products such as CO_2 and NH_3 from —COOH and —NH_2 groups of ALA were formed from the thermal degradation of ALA when ALA was catalyzed by solid acid sites, as previously reported [26]. The gaseous products were estimated using red litmus test papers and $CaCl_2$ for NH_3 and CO_2, respectively. The mixed indicator contained 1% bromocresol green ethanol solution and 2% methyl red ethanol solution with a volume ratio of 3:1; the color of the indicator changed from red to green when the pH value of the solution was greater than 5.1 [28–30].

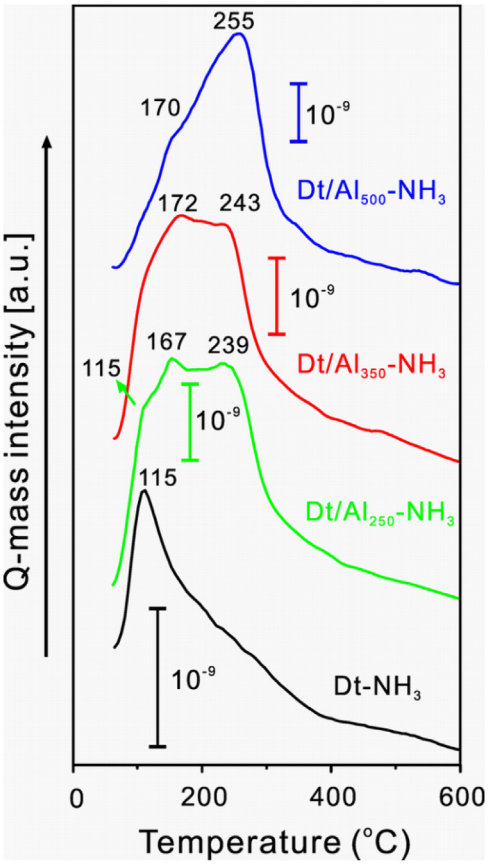

Fig. 1. TPD curves of the desorbed NH_3 of Dt and its Al-incorporated products.

3. Results and discussion

Only one band centered at 115 °C was clearly distinguished in the TPD curve of Dt-NH_3 over the temperature range of 60–600 °C (Fig. 1). The band was attributed to the desorption signal of acid-bound NH_3, and the acid sites were mainly Si-OHs from diatomite. The low NH_3 desorption temperature indicates the weak acidity of diatomite. The 115 °C band has a shoulder band in the curve of the Al-incorporated diatomite that was obtained by heating at 250 °C (Dt/Al_{250}–NH_3, Fig. 1). This band for Dt/Al_{350}–NH_3 is hardly distinguished and is not observed in the curve of Dt/Al_{500}–NH_3. The weakening and disappearance of this NH_3-desorption band for Al-incorporated diatomite is attributed to the decrease in number of diatomite Si-OHs, which react with Al_{13} hydroxyl groups, as revealed by ^{29}Si MAS NMR spectra (see our previous report [24]).

Compared with the TPD curves of Dt-NH_3, those of the NH_3-adsorped diatomite after the Al incorporation exhibit two new NH_3-adsorption bands, which are centered at approximately 167 °C and 239 °C for Dt/Al_{250}–NH_3, 172 °C and 243 °C for Dt/Al_{350}–NH_3, and 170 °C and 255 °C for Dt/Al_{500}–NH_3 (Fig. 1). These two bands are assigned to the NH_3 desorption of B (Al-OHs) and L (unsaturated Al^{3+} ions, which are denoted here as Al-) acid sites from Al_{13} [24,31]. In the case of samples heated at ≥350 °C, the number of B acid sites decreased because of the dehydroxylation of Al-OHs of Al_{13}, whereas unsaturated Al^{3+} ions formed and the number of L acid sites (Al-) consequently increased [24,32]. L acid sites were predominant when Al was incorporated into the structure of diatomite and heated at 500 °C, as displayed in the FTIR spectra in our previous study [24]. Therefore, the 255 °C band, which is the predominant band in the TPD curve of Dt/Al_{500}–NH_3, is attributed to the desorption band of NH_3 bound to L acid sites. The 170 °C band is attributed to the desorption of B-acid-site-bound NH_3. Given that NH_3 bound to B acid sites exhibits a lower desorption temperature than that bound to L acid sites, the L acidity is stronger than the B acidity. That is, the acidity of Al- is stronger than that of Al-OHs, as estimated using NH_3 as the probed molecule. Furthermore, the relative areas of the corresponding bands of desorbed NH_3 were used to evaluate the numbers of acid sites. As shown in Fig. 1, the relative area of the NH_3-desorption band markedly increased after Al incorporation, and the relative areas of NH_3 desorption bands of Dt/Al_{250}–NH_3, Dt/Al_{350}–NH_3 and Dt/Al_{500}—NH_3 were similar. This result indicates that the solid acid amount increased after the Al incorporation, and that the total number of acid sites remained nearly constant, despite the differences in preparation temperatures of Al-incorporated diatomite. The former result is a consequence of the introduction of Al-OHs and Al-, and the latter result is due to the transformation of B acid sites (Al-OHs) into L acid sites (Al-) via the dehydroxylation of Al_{13} after heating, consistent with the FTIR and ^{29}Si MAS NMR spectra results reported in our previous work [24].

Pure ALA began to decompose at temperatures above 200 °C, with a small DTG peak at 214.2 °C (see Supporting information, Fig. S1). The major thermal event of pure ALA occurred in the range of 400–550 °C and resulted in a sharp DTG peak at 464.0 °C. Some weak B acid sites of diatomite from Si-OHs are present [5], and these sites induced the catalytic decomposition of ALA and decreased the decomposition temperature from 464.0 to 450.1 (Dt-ALA, Fig. 2). The weak DTG peak centered at 467.4 °C is attributed to ALA molecules that did not contact the acid sites of diatomite. The decomposition temperature of ALA considerably decreased by more than 30 °C to 430.3 °C for Dt/Al_{250}-ALA, which shows that the incorporated Al_{13} exhibits higher catalytic activity than diatomite. A higher preparation temperature of Al-incorporated diatomite corresponds to a lower decomposition temperature of ALA for the ALA-modified diatomite complex. Dt/Al_{500}-ALA exhibited the lowest decomposition temperature of ALA, which was only 405.8 °C (Fig. 2). As previously mentioned, L acid sites are predominant in Dt/Al_{500}, which indicates that the Al-incorporated diatomite with mainly L acid sites exhibits much higher catalytic activity than that with coexistence of B and L acid sites. Therefore, L acid sites are more effective than B acid sites in catalyzing the ALA decomposition.

The gaseous products of the thermal degradation of pure ALA could not change the red color of litmus test papers to blue, which implies a lack of NH_3. Notably, the $CaCl_2$ solution became turbid after the injection of gaseous products; however, no precipitate appeared when pure ALA was heated at approximately 450 °C, which implies that few CO_2 molecules were produced during the degradation of pure ALA. By contrast, the color of the litmus test paper changed from red to blue after the gaseous products of the diatomite-ALA complex appeared. As observed in our previous catalysis experiments involving ALA degradation, the B acid sites of montmorillonite catalyzed ALA to generate NH_3 via the Hofmann elimination pathway [27]. Similarly, B acid sites (Si-OHs) from diatomite promote the breakage of the C—N bond of ALA to form NH_3. Moreover, precipitates appeared when the gaseous products of the diatomite-ALA composite, which were obtained at approximately 430 °C, were injected into the $CaCl_2$ solution. These results indicate that diatomite-ALA formed more CO_2 molecules than pure ALA because of the catalysis of L acid sites [27], which originated from the clay mineral impurity of diatomite [20,24].

Similarly, all Al-incorporated diatomite-ALA products produced NH_3 when ALA degraded under catalysis by B acid sites (Al-OHs). More CO_2 molecules were generated from the degradation of Al-incorporated diatomite-ALA prepared at higher temperatures, which induces greater precipitation in the $CaCl_2$ solution. These results indicate that the number of L acid sites (Al-) increases with increasing preparation temperature of Al-incorporated diatomite,

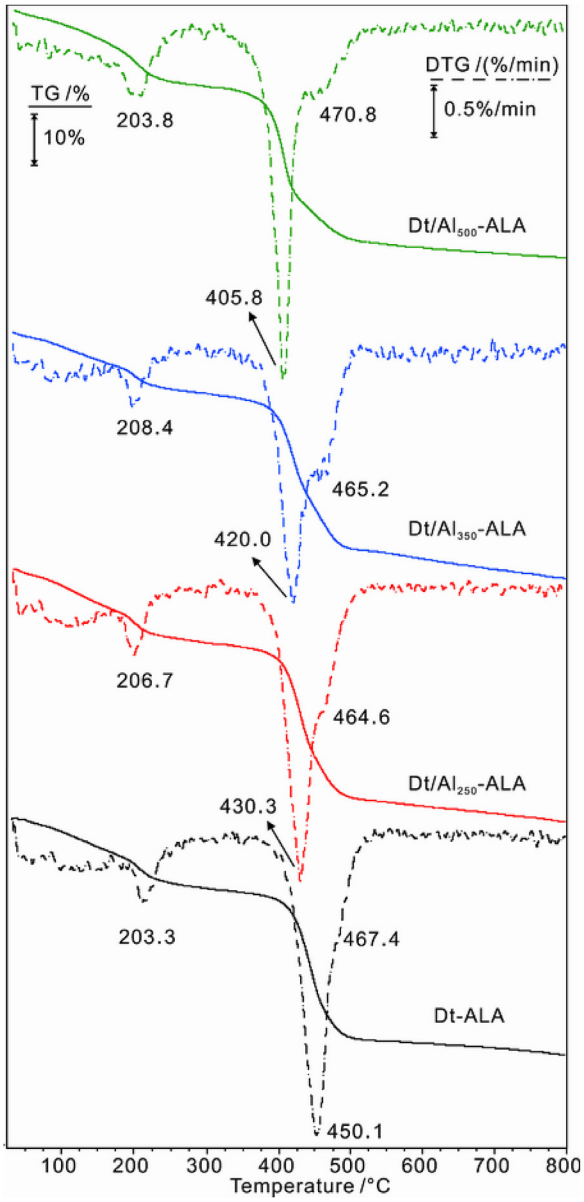

Fig. 2. TG and DTG curves of the ALA-diatomite complex and the ALA-modified diatomite complexes.

consistent with the TPD results. The formation temperatures of NH_3 and CO_2 are approximately 435 °C and 405 °C, respectively, for Al-incorporated diatomite-ALA, which indicates that the catalysis reaction of L acid sites for ALA degradation begins earlier than that of B acid sites in Al-incorporated diatomite.

4. Conclusions

Al incorporation markedly enhances the solid acidity of diatomite, as demonstrated by the simultaneous increase in number of B (Al-OHs) and L (Al-) acid sites from the implanted Al_{13}. The TPD results show that the number of L acid sites increases with increasing preparation temperature of Al-incorporated diatomite because of the transformation of B to L acid sites via dehydroxylation after heating. Moreover, L acid sites exhibit a higher NH_3 desorption temperature than B acid sites, which indicates that L acid sites are more acidic than B acid sites.

Al-incorporated diatomite exhibits high catalytic activity and considerably decreases the degradation temperature of ALA. The B acid sites catalyze ALA to generate NH_3 by promoting the breakage of the C—N bond of ALA to form NH_3 (Hofmann elimination pathway), and the L acid sites can catalyze ALA to form CO_2. CO_2 has a lower generation temperature than NH_3.

Acknowledgements

The financial supports from the Natural Science Foundation for Distinguished Young Scientists of Guangdong Province (Grant No. 2016A030306034), National Natural Scientific Foundation of China (Grant No. 41202024), Science and Technology Program of Guangzhou, China (Grant No. 201510010138), and the CASSAFEA International Partnership Program for Creative Research Teams (Grant No. 20140491534) are gratefully acknowledged. This is a contribution (No.IS-2294) from GIGCAS.

Appendix A. Supplementary data

Supplementary data associated with this article can be found, in the online version, at http://dx.doi.org/10.1016/j.colsurfa.2016.09.005.

References

[1] E.M. Bens, C.M. Drew, Diatomaceous earth: scanning electron microscope of 'Chromosorb P', Nature 216 (1967) 1046–1048.
[2] D. Losic, J.G. Mitchell, N.H. Voelcker, Diatomaceous lessons in nanotechnology and advanced materials, Adv. Mater. 21 (2009) 2947–2958.
[3] P. Yuan, D.Q. Wu, Z. Chen, Z.W. Chen, Z.Y. Lin, G.Y. Diao, J.L. Peng, H^1 MAS NMR spectra of hydroxyl species on diatomite surface, Chin. Sci. Bull. 46 (2001) 1118–1121.
[4] P. Yuan, D.Q. Wu, Z.Y. Lin, G.Y. Diao, J.L. Peng, J.F. Wei, Study on the surface hydroxyl species of diatomite using DRIFT Spectroscopy, Spectrosc. Spectr. Anal. 21 (2001) 783–786.
[5] P. Yuan, D.Q. Wu, H.P. He, Z.Y. Lin, The hydroxyl species and acid sites on diatomite surface: a combined IR and Raman study, Appl. Surf. Sci. 227 (2004) 30–39.
[6] D. Losic, J.G. Mitchell, R. Lal, N.H. Voelcker, Rapid fabrication of micro- and nanoscale patterns by replica molding from diatom biosilica, Adv. Funct. Mater. 17 (2007) 2439–2446.
[7] M. Sprynskyy, T. Kowalkowski, H. Tutu, E.M. Cukrowska, B. Buszewski, Ionic liquid modified diatomite as a new effective adsorbent for uranium ions removal from aqueous solution, Colloids Surf. A 465 (2015) 159–167.
[8] Q. Zhou, H. Yang, C. Yan, W. Luo, X. Li, J. Zhao, Synthesis of carboxylic acid functionalized diatomite with a micro-villous surface via UV-induced graft polymerization and its adsorption properties for Lanthanum(III) ions, Colloids Surf. A 501 (2016) 9–16.
[9] M.A.M. Khraisheh, M.A. Al-Ghouti, S.J. Allen, M.N. Ahmad, Effect of OH and silanol groups in the removal of dyes from aqueous solution using diatomite, Water Res. 39 (2005) 922–932.
[10] W. Yu, L. Deng, P. Yuan, D. Liu, W. Yuan, P. Liu, H. He, Z. Li, F. Chen, Surface silylation of natural mesoporous/macroporous diatomite for adsorption of benzene, J. Colloid Interface Sci. 448 (2015) 545–552.
[11] G. Sheng, S. Wang, J. Hu, Y. Lu, J. Li, Y. Dong, X. Wang, Adsorption of Pb (II) on diatomite as affected via aqueous solution chemistry and temperature, Colloids Surf. A 339 (2009) 159–166.
[12] W. Yuan, P. Yuan, D. Liu, W. Yu, L. Deng, F. Chen, Novel hierarchically porous nanocomposites of diatomite-based ceramic monoliths coated with silicalite-1 nanoparticles for benzene adsorption, Microporous Mesoporous Mater. 206 (2015) 184–193.
[13] H. Hadjar, B. Hamdi, M. Jaber, J. Brendlé, Z. Kessaïssia, H. Balard, J.B. Donnet, Elaboration and characterisation of new mesoporous materials from diatomite and charcoal, Microporous Mesoporous Mater. 107 (2008) 219–226.
[14] Z. Bao, E.M. Ernst, S. Yoo, K.H. Sandhage, Syntheses of porous self-supporting metal-nanoparticle assemblies with 3D morphologies inherited from biosilica templates (Diatom frustules), Adv. Mater. 21 (2009) 474–478.
[15] L. Zheng, C. Wang, Y. Shu, X. Yan, L. Li, Utilization of diatomite/chitosan-Fe (III) composite for the removal of anionic azo dyes from wastewater: equilibrium, kinetics and thermodynamics, Colloids Surf. A 468 (2015) 129–139.
[16] T. Datsko, V. Zelentsov, E. Dvornikova, Physicochemical and adsorption-structural properties of diatomite modified with aluminum compounds, Surf. Eng. Appl. Electrochem. 47 (2011) 530–539.
[17] W. Yu, P. Yuan, D. Liu, L. Deng, W. Yuan, B. Tao, H. Cheng, F. Chen, Facile preparation of hierarchically porous diatomite/MFI-type zeolite composites and their performance of benzene adsorption: the effects of NaOH etching pretreatment, J. Hazard. Mater. 285 (2015) 173–181.
[18] W. Yuan, P. Yuan, D. Liu, W. Yu, M. Laipan, L. Deng, F. Chen, In situ hydrothermal synthesis of a novel hierarchically porous TS-1/modified-diatomite composite for methylene blue (MB) removal by the

synergistic effect of adsorption and photocatalysis, J. Colloid Interface Sci. 462 (2016) 191–199.
[19] S. Holmes, B. Graniel-Garcia, P. Foran, P. Hill, E. Roberts, B. Sakakini, J. Newton, A novel porous carbon based on diatomaceous earth, Chem. Commun. (2006) 2662–2663.
[20] D. Liu, P. Yuan, D. Tan, H. Liu, M. Fan, A. Yuan, J. Zhu, H. He, Effects of inherent/enhanced solid acidity and morphology of diatomite templates on the synthesis and porosity of hierarchically porous carbon, Langmuir 26 (2010) 18624–18627.
[21] D. Liu, P. Yuan, D.Y. Tan, H.M. Liu, T. Wang, M.D. Fan, J.X. Zhu, H.P. He, Facile preparation of hierarchically porous carbon using diatomite as both template and catalyst and methylene blue adsorption of carbon products, J. Colloid Interface Sci. 388 (2012) 176–184.
[22] D. Liu, W. Yuan, L. Deng, W. Yu, H. Sun, P. Yuan, Preparation of porous diatomite-templated carbons with large adsorption capacity and mesoporous zeolite KH as a byproduct, J. Colloid Interface Sci. 424 (2014) 22–26.
[23] D. Liu, W. Yuan, P. Yuan, W. Yu, D. Tan, H. Liu, H. He, Physical activation of diatomite-templated carbons and its effect on the adsorption of methylene blue (MB), Appl. Surf. Sci. 282 (2013) 838–843.
[24] D. Liu, W. Yu, L. Deng, W. Yuan, L. Ma, P. Yuan, P. Du, H. He, Possible mechanism of structural incorporation of Al into diatomite during the deposition process I. Via a condensation reaction of hydroxyl groups, J. Colloid Interface Sci. 461 (2016) 64–68.
[25] S. Jiyang, X. Mingju, Q. Dingchuang, Z. Youping, Significance of amino acids and fatty acids for the formation of the bio-thermocatalytic transition zone gases, Acta Sedimentol. Sin. 2 (1995).
[26] H. Liu, P. Yuan, Z. Qin, D. Liu, D. Tan, J. Zhu, H. He, Thermal degradation of organic matter in the interlayer clay–organic complex: a TG-FTIR study on a montmorillonite/12-aminolauric acid system, Appl. Clay Sci. 80 (2013) 398–406.
[27] H. Liu, P. Yuan, D. Liu, D. Tan, H. He, J. Zhu, Effects of solid acidity of clay minerals on the thermal decomposition of 12-aminolauric acid, J. Therm. Anal. Calorim. 114 (2013) 125–130.
[28] E. Conway, E. O'malley, Microdiffusion methods. Ammonia and urea using buffered absorbents (revised methods for ranges greater than 10 μg N), Biochem. J 36 (1942) 655.
[29] V. Quaschning, J. Deutsch, P. Druska, H.-J. Niclas, E. Kemnitz, Properties of modified zirconia used as friedel-crafts-acylation catalysts, J. Catal. 177 (1998) 164–174.
[30] D. Liu, P. Yuan, H. Liu, J. Cai, D. Tan, H. He, J. Zhu, T. Chen, Quantitative characterization of the solid acidity of montmorillonite using combined FTIR and TPD based on the NH 3 adsorption system, Appl. Clay Sci. 80 (2013) 407–412.
[31] K. Urabe, H. Sakurai, Y. Izumi, Cation-exchanged synthetic saponite as a 'heat-stable'acidic clay catalyst, Journal of the Chemical Society, Chem. Commun. (1988) 1520–1521.
[32] S. Bodoardo, F. Figueras, E. Garrone, IR study of Brönsted acidity of Al-pillared montmorillonite, J. Catal. 147 (1994) 223–230.